Group-Based Sparse Representation Based on ℓ_p-norm Minimization for Compressive Sensing

Ruijing Li, Yechao Bai, Xinggan Zhang, Lan Tang, and Qiong Wang
School of Electronic Science and Engineering, Nanjing University, Nanjing, China
Email: lrj@smail.nju.edu.cn, {ychbai, zhxg, tanglan, Wangqiong}@nju.edu.cn

***Abstract*—Sparse coding has been applied in various domains, especially in image restoration. Most methods depend on the ℓ_1-norm optimization techniques and the patch-based sparse representation models, but they suffer from two limits: one is the high computational complexity in dictionary learning; the other is ignoring the relationship among patches which influences the accuracy of sparse coding coefficients. In this paper, we choose the group-based sparse representation models to simple calculation process and realize the nonlocal self-similarity of images by graph-based transform dictionary design. Besides, we utilize ℓ_p-norm minimization to solve nonconvex optimization problems on the basis of the weighted schatten p-norm minimization, which can make the optimization model more flexible. Through reasonable parameters selection, experimental results show that our proposed method has a better performance on the compressive sensing than many current state-of-the-art schemes in both peak signal-to-noise ratio and visual perception.**

***Index Terms*—sparse coding, group-based sparse, ℓ_p-norm minimization, compressive sensing**

I. Introduction

Restoring a clean image from its degraded image has been widely studied by various methods [1]-[8] in recent years. Many image restoration problems can be mathematically modeled by:

$$\boldsymbol{Y} = \boldsymbol{HX} + \boldsymbol{N} \tag{1}$$

where $\boldsymbol{Y}$ and $\boldsymbol{X}$ denote the observed image and the original high-quality image respectively, $\boldsymbol{H}$ denotes a non-invertible linear operator, and $\boldsymbol{N}$ represents an additive Gaussian white noise.

The image restoration problem is settled by restoring the clean image $\boldsymbol{X}$ from the observed image $\boldsymbol{Y}$. For different choices of $\boldsymbol{H}$, (1) becomes different image processing problems [8], [9]. In this paper, $\boldsymbol{H}$ is a set of random projections, and we mainly deal with the compressive sensing problem, aiming at gray images.

To find a good solution to (1) with ill-posed nature, the following minimization problem is usually employed for regularizing the solution:

$$\widehat{X} = \arg\min_{X} \| \boldsymbol{Y} - \boldsymbol{H}X \|_2^2 + \lambda \Phi(X) \tag{2}$$

where $\| \boldsymbol{Y} - \boldsymbol{H}X \|_2^2$ is a ℓ_2-norm fidelity constraint, λ is the regularization parameter, and $\Phi(X)$ is called the regularization term denoting image prior. Many optimization approaches for the above regularization-based image inverse problems have been developed, which can be summarized as the following three stages of development.

The basic unit of an image is the pixel. Naturally, the initial researches on image restoration were based on pixels, where the most representative method is the total variation (TV) model [10]-[12]. However, the TV model damages the details of image and makes the images over-smooth. The better approaches that are considered at the patch level have been proposed, where the representative approaches are Gaussian mixture model (GMM) and Block-Matching 3D filtering (BM3D) [13]. But they suffer from some limits, like dictionary learning with great computational complexity. In order to solve the above problems, sparse representation based on the group appears. The group-based sparse representation model (GSR) [8] reduces the complexity and updates the noisy image iteratively.

In this paper, for the purpose of improving the problem solution more robust, we apply the ℓ_p-norm to solve nonconvex optimization problems. Inspired by the Weighted Schatten p-norm Minimization (WSNM) [14], we propose the group-based sparse representation based on ℓ_p-norm minimization (LPGSR). Experimental results illustrate that the proposed method has surpassed many latest methods.

The remainder of this paper is organized as follows. In Section II, we describe the group-based sparse representation. In Section III, we describe optimization for GSR-driven ℓ_p-norm minimization. The experimental results are presented in Section IV, and Section V concludes the paper.

II. Group-Based Sparse Representation

In the scenario of Image Restoration, what we observed is the degraded image $\boldsymbol{Y}$ via (1), and the aim is to recover the original image $\boldsymbol{X}$ from the degraded image $\boldsymbol{Y}$ by utilizing the proposed scheme.

Manuscript received November 18, 2019; revised February 27, 2020.

doi: 10.18178/ijsps.8.1.13-18

A. The Construction of a Group

In recent years, some advanced methods [8], [15] have shown that sparsity based on group performs powerfully in the image restoration.

In general, the establishment of the group can be divided into three stages, which are extracting, matching and stacking.

Step 1: The whole image with size N will be divided into n patches with size $\sqrt{d}\times\sqrt{d}$.

Step 2: In the size $\sqrt{L}\times\sqrt{L}$ searching window that contains the typical patch, we search for many similar patches that have similar image construct.

Step 3: All patches in the set will be stacked into a matrix. The matrix composed of all patches with similar structure is called a group.

According to the above definition, it is obvious to find that the construction of the group explicitly exploits the self-similarity of natural images.

B. Adaptive Dictionary Learning

Similar to patch-based sparse representation, given a dictionary $\boldsymbol{D}_i$, which is often learned from each group, each group $\boldsymbol{X}_i$ can be sparsely represented as $\boldsymbol{\alpha}_i = \boldsymbol{D}_i^{-1}\boldsymbol{X}_i$ and solved by the following ℓ_0 -norm minimization problem:

$$\boldsymbol{\alpha}_i = \arg\min_{\boldsymbol{\alpha}_i} \sum_{i=1}^{n} \left(\frac{1}{2}\| \boldsymbol{X}_i - \boldsymbol{D}_i\boldsymbol{\alpha}_i \|_F^2 + \lambda_i \| \boldsymbol{\alpha}_i \|_0\right) \quad (3)$$

where $\|\bullet\|_F^2$ denotes the Frobenious norm and λ_i is the regularization parameter. $\|\bullet\|_0$ is ℓ_0 -norm, counting the nonzero entries of $\boldsymbol{\alpha}_i$.

In the self-adaptive dictionary learning, for each group $\boldsymbol{X}_i$, its adaptive dictionary can be learned from its observation $\boldsymbol{Y}_i \in \mathbb{R}^{d\times k}$.

For a given patch of size $\sqrt{d}\times\sqrt{d}$, we firstly search for its K-nearest-neighbors (KNN). The aim is to find the K most similar patches. The KNN together with the exemplar patch is called a group in the sequel. We then stack them as columns to create a data matrix $\boldsymbol{Y}$. Similar to BM3D [16], the K most similar patches to the exemplar patch are found using block-matching and Euclidean distance.

We learn the graph-based transform dictionary for similar patches by exploiting their common structure. Specifically, we compute an average patch, from which a similarity graph is constructed modeling the local neighborhood correlations among pixels. There are different flavors of similarity graphs, such as K-nearest neighbor graph and the fully connected graph [17]. For the sake of simplicity, we choose a graph where only pairwise adjacent pixels are connected. In particular, we construct an undirected weighted graph by treating each pixel in the average patch as a node and connect adjacent pixels (i, j) with edge weight:

$$\omega_{i,j} = e^{\frac{-\|y_i - y_j\|^2}{\sigma_\omega^2}} \quad (4)$$

where $\|y_i\text{-}y_j\|^2$ calculates the squared intensity difference in pixel i and j as a measure of similarity. The parameter σ_ω controls the sensitivity of the similarity measure to the noise and the range of the intensity difference.

III. Optimization for GSR-Driven P-Norm Mimimization

In this section, an efficient approach is developed to solve the proposed GSR-driven ℓ_p -norm minimization for image restoration, which is one of our main contributions.

A. Non-convex Approximation

A series of approximation for image restoration are non-convex and NP-hard. The traditional methods apply ℓ_1 -norm minimization to solve the image restoration problem [18]. However, for some practical problems including image inverse problems, the conditions describing the equivalence of image restoration problems and ℓ_1 -norm minimization are not necessarily satisfied.

To deal with the limitations, we introduce the original p-norm $(\sum_i \sigma_i^p)^{1/p}$ with $0 < p \le 1$. Most of the p-norm based models treat all singular values equally, but they are not flexible enough to deal with many real problems where different rank components have different importance. In order to solve the problem, we apply the Weighted Schatten p-Norm Minimization (WSNM) which assigns different weights to different singular values. As a result, we define a new weighted p-norm of a matrix $\mathrm{X} \in \mathbb{R}^{m\times n}$, which is defined as:

$$\|\mathbf{X}\|_{\mathbf{w},\mathrm{S}_p} = \left(\sum_{i=1}^{\min\{m,n\}} \omega_i \sigma_i^p\right)^{\frac{1}{p}} \quad (5)$$

where $\mathbf{w}=[\omega_1, ..., \omega_{\min\{m,n\}}]$ is a non-negative vector, ω_i is a non-negative weight assigned to σ_i, and σ_i is the i-th singular value of $\mathbf{X}$.

Then the weighted p-norm of $\mathbf{X}$ with power p is:

$$\|\mathbf{X}\|_{\mathbf{w},\mathbf{S}_p}^p = \sum_{i=1}^{\min\{m,n\}} \omega_i \sigma_i^p = tr(\mathbf{W}\Delta^p) \quad (6)$$

where both $\mathbf{W}$ and Δ are diagonal matrices whose diagonal entries are composed of ω_i and σ_i, respectively.

For a given dictionary $\boldsymbol{D}_i$, the sparse coding of each group $\boldsymbol{X}_i$ can be represented as $\boldsymbol{X}_i = \boldsymbol{D}_i\boldsymbol{\alpha}_i$, where $\boldsymbol{\alpha}_i$ is a sparse vector that the coefficients are zero or close to zero.

The image restoration for recovering the original image $\boldsymbol{X}$ from $\boldsymbol{Y}$ will be dealt with solving the following non-convex p-norm minimization problem:

$$\boldsymbol{\alpha} = \arg\min_{\boldsymbol{\alpha}} \frac{1}{2}\| \boldsymbol{Y} - \boldsymbol{H}\boldsymbol{D}\boldsymbol{\alpha} \|_2^2 + \lambda \| \boldsymbol{\omega}\boldsymbol{\alpha} \|_p . \quad (7)$$

Given a matrix $\boldsymbol{Y}$, our proposed LPGSR model aims to find a matrix $\boldsymbol{X}$ which is as close to $\boldsymbol{Y}$ as possible under the F-norm data fidelity and the weighted Schatten p-norm regularization:

$$\widehat{\boldsymbol{X}}=\arg\min_{\boldsymbol{X}} \| \boldsymbol{X}-\boldsymbol{Y} \|_F^2 +\lambda \| \boldsymbol{X} \|_{\mathbf{w},S_p}^p \quad (8)$$

where λ is a tradeoff parameter to balance the data fidelity and regularization.

Under the adaptive dictionary design, for a matrix $\boldsymbol{Y}_i$ with nonlocal similar patches, the corresponding estimate $\boldsymbol{X}_i$ of the original image can be defined as the following optimization problem:

$$\widehat{\boldsymbol{X}}_i=\arg\min_{\boldsymbol{X}_i} \frac{1}{\sigma_n^2} \| \boldsymbol{X}_i-\boldsymbol{Y}_i \|_F^2 + \| \boldsymbol{X}_i \|_{\mathbf{w},S_p}^p \quad (9)$$

where σ_n^2 denotes the noise variance of additive white Gaussian noise.

Obviously, it is important to analyze the suitable setting of power p for each noise level σ_n according to (9) in our proposed method. Therefore, we choose 3 images from Fig. 1 randomly and add noise to them, and then test the proposed method with different power p under the various levels of noise. When handling low and medium noise levels, the best values of p are big. But when the noise level becomes stronger, the smaller values of p are preferred.

B. Split Iteration Algorithm

1) Iterative sub-problems

Since it is a large scale non-convex optimization problem, solving the objective function of (7) is very difficult. To make the proposed scheme tractable and robust, in this paper we apply the split iteration [15] to solve (7). More specifically, by introducing an auxiliary variable $\boldsymbol{Z}$ whose form is $\boldsymbol{Z}=\boldsymbol{D\alpha}$, we firstly transform (7) into an equivalent constrained form:

$$\boldsymbol{\alpha}=\arg\min_{\boldsymbol{Z},\boldsymbol{\alpha}} \frac{1}{2} \| \boldsymbol{Y}-\boldsymbol{HZ} \|_2^2 +\lambda \| \boldsymbol{\omega\alpha} \|_p, s.t. \boldsymbol{Z}=\boldsymbol{D\alpha} \quad (10)$$

The parameter ρ is fixed to avoid the problem of numerical instability, rather than selecting a predefined sequence that tends to infinity. Then, we have

$$\boldsymbol{Z}^{t+1}=\arg\min_{\boldsymbol{Z}} \frac{1}{2} \| \boldsymbol{Y}-\boldsymbol{HZ} \|_2^2 +\frac{\rho}{2} \| \boldsymbol{Z}-\boldsymbol{D\alpha}^t-\boldsymbol{C}^t \|_2^2 \quad (11)$$

$$\boldsymbol{\alpha}^{t+1}=\arg\min \lambda \| \boldsymbol{\omega\alpha} \|_p +\frac{\rho}{2} \| \boldsymbol{Z}^{t+1}-\boldsymbol{D\alpha}-\boldsymbol{C}^t \|_2^2 \quad (12)$$

and

$$\boldsymbol{C}^{t+1}=\boldsymbol{C}^t-(\boldsymbol{Z}^{t+1}-\boldsymbol{D\alpha}^{t+1}) \quad (13)$$

Therefore, it is obvious to see that the minimization for (10) has been transformed into two splitting minimization sub-problems, which are $\boldsymbol{Z}$ and $\boldsymbol{\alpha}$ sub-problems. Each sub-problem minimization can be much easier than the original problem.

2) Threshold setting

Each subproblem can be solved by the generalized soft-thresholding (GST) [19] algorithm effectively. Given p and ω_i, a specific threshold can be calculated:

$$\tau_p^{GST}(\omega_i)=(2\omega_i(1-p))^{\frac{1}{2-p}}+\omega_i p(2\omega_i(1-p))^{\frac{p-1}{2-p}} \quad (14)$$

When the condition $\sigma_i<\tau_p^{GST}(\omega_i)$ is met, the iterative process continues.

The generalized soft-thresholding function is shown as follow:

$$S_p^{GST}(\sigma_i;\omega_i)=\begin{cases}0, if\ \sigma_i \le \tau_p^{GST}(\omega_i)\\ \mathrm{sgn}(\sigma)\delta^{(k)}, if\ \sigma_i > \tau_p^{GST}(\omega_i)\end{cases} \quad (15)$$

where δ_i is an element in $\Delta=diag(\delta_1,...,\delta_r)$ of $\boldsymbol{X}=\boldsymbol{U}\Delta\boldsymbol{V}^T$.

IV. Experiment Results

In this section, we use 18 images that are shown in Fig. 1 to test the performance of the proposed models. The performance of the proposed model can refer to several values, mainly aiming at peak signal-to-noise ratio (PSNR, unit: dB) and feature similarity (FSIM, range: (0, 1)). To measure the quality of the processed image, we usually refer to the PSNR value to measure the satisfaction of a certain process, which is an objective criterion for evaluating images. FSIM is a proposed powerful perceptual quality metric to evaluate the visual quality recently, whose higher value means the better visual quality.

Figure 1. All experimental test images.

In image compressive sensing recovery, we generated the compressive sensing measurements at the block level by utilizing a Gaussian random projection matrix to test images, where the block size is 32×32. The size of each patch $\sqrt{d}\times\sqrt{d}$ is set to be 7×7. And similar patch numbers are set to be 60.

We use the single variable method to ensure the rigor of the experimental results. For the cases of different measurements, when the p value is determined, the optimal value setting of the corresponding parameter is also determined. The specific experimental content is as follows.

A. p Value in the ℓ_p-norm

It can be known from the reference [19] that the selection of the p value in the ℓ_p-norm can have some special values, such as 1/2, 2/3. However, in reference [14], we can see that the selection of p values can be varied, not limited to the selection of a few special values. The best value of power p is inversely proportional to the noise level. With the noise level becoming stronger, the value of p becomes smaller. More specifically, when

handling low and medium noise levels (40, 50 and 60), the best values of p are 0.8, 0.75 and 0.75, respectively. And the p values of 0.1, 0.05 and 0.05 are for noise levels 70, 80 and 90, respectively. The Fig. 2 has shown the influence of changing p upon denoised results under different noise levels. Similarly, in the case of high measurements, the p value is relatively large, and in the case of low measurements, the p value is relatively small. In this paper, the values of p parameter are set to 0.05 in the cases of 10% and 20% measurements, to 0.1 in 30%, and to 0.75 in the case of 40% measurements.

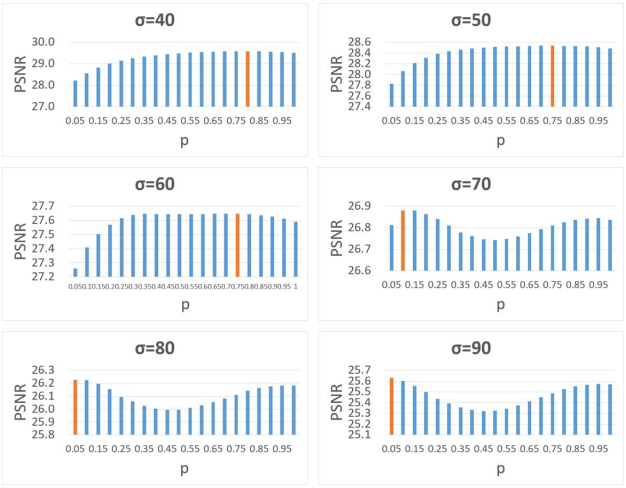

Figure 2. The influence of changing p upon denoised results under different noise levels.

B. Experimental Comparison

In the case of basic parameter settings, we perform an overall test of 18 images in Fig. 1 in the cases of different measurements. In Table I, we randomly select 9 images for display.

TABLE I. PSNR AND FSIM COMPARISONS WITH DIFFERENT METHODS IN THE CASE OF 10% MEASUREMENTS

Image	Method			
	TVNLR	BD3D	GSR	LPGSR
Man	23.43/0.774	22.53/0.787	23.63/**0.830**	**24.08**/0.823
Monarch	23.37/0.842	23.23/0.809	25.29/0.867	**25.86**/**0.877**
Pentagon	22.26/0.707	21.87/0.744	23.06/**0.811**	**23.21**/0.789
Peppers	25.62/0.846	25.56/0.860	26.91/0.886	**27.55**/**0.891**
Starfish	22.90/0.793	20.72/0.759	23.60/0.839	**24.26**/**0.853**
Tank	28.85/0.791	28.28/0.818	28.87/**0.832**	**29.37**/0.829
Cameraman	23.08/0.799	**24.99**/**0.836**	22.90/0.815	23.58/0.820
Couple	24.12/0.760	23.04/0.764	24.55/**0.840**	**25.02**/0.822
Girl	30.54/0.849	29.59/0.856	31.28/**0.881**	**31.32**/0.880

The proposed LPGSR is compared with recent representative methods of pixel, patch and group on compressive sensing, which are TV based image compressive sensing recovery algorithm by nonlocal regularization (TVNLR), block-matching 3D (BM3D), and group-based sparse representation (GSR). TVNLR introduces a new NLM based non-local regularization constraint for the first time. BM3D replaces the traditional parametric modeling used in compressive sensing by a non-parametic one. GSR exploits the concept of group as the basic unit of sparse representation, and establishes a novel sparse representation modeling of natural images.

The visual quality comparisons of compressive sensing in the case of only 10% measurements are shown from Fig. 3 to Fig. 4. We take the cases of two different standard gray test images which are *Monarch* and *Peppers* contained in Fig. 1 as examples. It is obvious to see that LPGSR does well in providing better compressive sensing effects on both edges and textures compared with TVNLR, BM3D and GSR. For the image *Peppers*, the average PSNR value of the proposed scheme LPGSR over TVNLR, BM3D and GSR methods can be as much as 1.9317dB, 1.9859dB and 0.6386dB.

Figure 3. Visual quality comparison of image compressive sensing recovery on gray image *Monarch* in the case of ratio = 10%. From left to right: the compressive sensing recovered images by TVNLR (PSNR = 23.3656dB; FSIM = 0.84176), BM3D (PSNR = 23.2302dB; FSIM = 0.80931), GSR (PSNR = 25.2898dB; FSIM = 0.86733) and the proposed lp-GSR (PSNR = **25.8605**dB; FSIM = **0.87725**).

Figure 4. Visual quality comparison of image compressive sensing recovery on gray image *Peppers* in the case of ratio = 10%. From left to right: the compressive sensing recovered images by TVNLR (PSNR = 25.6151dB; FSIM = 0.84621), BM3D (PSNR = 25.5609dB; FSIM = 0.85951), GSR (PSNR = 26.9082dB; FSIM = 0.88569) and the proposed lp-GSR (PSNR = **27.5468**dB; FSIM = **0.89123**).

Because of the improvement of adaptive dictionary learning and different p values' setting for cases of different measurements, LPGSR has a better image recovery effect. To sum up, the proposed method not only removes most of the visual artifacts, but also reserves largescale sharp edges and small-scale fine image details more effectively. Experimental results indicate that the proposed modeling has a better performance than many current schemes, both in PSNR and FSIM visual perception.

V. CONCLUSION

In this paper, a group-based sparse representation based on ℓ_p -norm minimization model (LPGSR) is presented. LPGSR has two major merits: one is that simples the calculation process and reduces complexity; the other is that makes the optimization model more flexible than ℓ_1-norm minimization. Experimental results have shown that the proposed LPGSR achieves significant performance improvements on the compressive sensing over many current state-of-the-art schemes both in PSNR and FSIM. In the future, we will

extend the proposed LPGSR to other applications such as facial deblur, face recognition and so on.

CONFLICT OF INTEREST

The authors declare no conflict of interest.

AUTHOR CONTRIBUTIONS

Ruijing Li conceived the idea and conducted the numerical simulations and theoretical analysis. Yechao Bai and Lan Tang implemented data simulation processing. Ruijing Li, Yechao Bai, Xinggan Zhang, Lan Tang and Qiong Wang wrote the paper. All authors participated in the experiments and data analysis and read the paper. All authors had approved the final version.

ACKNOWLEDGMENT

The authors wish to thank Xinggan Zhang Professor, Yechao Bai Associate Professor and the other Professors for their constructive suggestions to improve the manuscript.

REFERENCES

[1] R. Li, S. Osher, and E. Fatemi, "Nonlinear total variation based noise removal algorithms," in *Proc. 11th Annual International Conf of the Center for Nonlinear Studies on Experimental Mathematics: Computational Issues in Nonlinear Science*, 1992, pp. 259-268.
[2] A. Chambolle, "An algorithm for total variation minimization and applications," in *Proc. 4th Conference on Mathematics and Image Analysis*, Paris, 2004, pp. 89-97.
[3] E. Michael and A. Michal, "Image denoising via sparse and redundant representations over learned dictionaries," *IEEE Trans. on Image Processing*, vol. 4, pp. 3736-3745, Dec. 2006.
[4] G. Manu and A. Muthuvel, "Fast total variation based image restoration under mixed Poisson-Gaussian noise model," in *Proc. 15th IEEE International Symposium on Biomedical Imaging*, Washington, 2018, pp. 1264-1267.
[5] D. Aram, K. Vladimir, and E. Karen, "BM3D frames and variational image deblurring," *IEEE Trans. on Image Processing*, vol. 21, pp. 1715-1728, Apr. 2012.
[6] N. Milad, R. Hossein, and B. Massoud, "Image restoration using gaussian mixture models with spatially constrained patch clustering," *IEEE Trans. on Image Processing*, vol. 24, pp. 3624-3636, Nov. 2015.
[7] P. Vardan and E. Michael, "Multi-scale patch-based image restoration," *IEEE Trans. on Image Processing*, vol. 25, pp. 249-261, Jan. 2016.
[8] Z. Jian, Z. Debin, and G. Wen, "Group-based sparse representation for image restoration," *IEEE Trans. on Image Processing*, vol. 23, pp. 3336-3351, Aug. 2014.
[9] D. Weisheng, S. Guangming, and L. Xin, "Nonlocal image restoration with bilateral variance estimation: A low-rank approach," *IEEE Trans. on Image Processing*, vol. 22, pp. 700-711, Feb. 2013.
[10] B. S. Derin, M. Rafael, and K. K. Aggelos, "Total variation super resolution using a variational approach," in *Proc. 15th IEEE International Conference on Image Processing*, San Diego, 2008, pp. 641-644.
[11] J. P. Oliveira, J. M. Bioucas-Dias, and M. A. T. Figueiredo, "Adaptive total variation image deblurring: A majorization-minimization approach," *Signal Processing*, vol. 89, pp. 1683-1693, Sep. 2009.
[12] M. Lysaker and X. C. Tai, "Iterative image restoration combining total variation minimization and a second-order functional," *International Journal of Computer Vision*, vol. 66, pp. 5-18, 2006.
[13] K. Egiazarian, A. Tbi, and H. Katkovnik, "Compressed sensing image reconstruction via recursive spatially adaptive filtering," in *Proc. IEEE International Conference on Image Processing (ICIP 2007)*, San Antonio, 2007, pp. 549-552.
[14] Y. Xie, S. Gu, Y. Liu, W. Zuo, W. Zhang, and L. Zhang, "Weighted schatten p-Norm minimization for image denoising and background subtraction," *IEEE Trans. on Image Processing*, vol. 25, pp. 4842-4857, Oct. 2016.
[15] J. Zhang, D. Zhao, R. Xiong, S. Ma, and W. Gao, "Image restoration using joint statistical modeling in a space-transform domain," *IEEE Trans. on Circuits and Systems for Video Technology*, vol. 24, pp. 915-928, Jun. 2014.
[16] K. Dabov, A. Foi, V. Katkovnik, and K. Egiazarian, "Image denoising by sparse 3-D transform-domain collaborative filtering," *IEEE Trans. on Image Processing*, vol. 16, pp. 2080-2095, 2007.
[17] U. V. Luxburg, "A tutorial on spectral clustering," *Statistics and Computing*, vol. 17, pp. 395-416, Dec. 2007.
[18] A. Beck and M. Teboulle, "Fast gradient-based algorithms for constrained total variation image denoising and deblurring problems," *IEEE Trans. on Image Processing*, vol. 18, pp. 2419-2434, Nov. 2009.
[19] W. Zuo, D. Meng, L. Zhang, X. Feng, and D. Zhang, "A generalized iterated shrinkage algorithm for non-convex sparse coding," in *Proc. IEEE International Conference on Computer Vision*, Sydney, 2013, pp. 217-224.

Ruijing Li received the B.S. degree in electronic information engineering from Harbin Engineering University, Harbin, China, in 2017. Now she is currently pursuing the Ph.D. degree in information and communication engineering in Nanjing University, Nanjing, China. She has been awarded the first-class scholarship for two consecutive years during the postgraduate period, and she is studying for the doctor's degree in advance. Her current research interests include image processing, target recognition and machine learning.

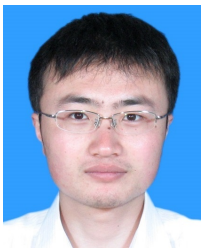

Yechao Bai received the B.S. and the Ph.D. degrees in electronic science and engineering from Nanjing University, Nanjing, China, in 2005 and 2010, respectively. Since 2010, he has been with Nanjing University, where he is currently an Associate Professor with the School of Electronic Science and Engineering. In the field of radar and array signal processing, He has published more than 50 academic papers, of which 30 were retrieved by SCI and EI. His current research interests include array signal processing and parameter estimation.

Xinggan Zhang received the B.S. degree in electrical engineering and the S.M. and Ph.D. degrees from the Nanjing University of Aeronautics and Astronautics (NUAA), Nanjing, China, in 1982, 1988, and 2001, respectively. In 1992, he joined the Department of Electronic Engineering, NUAA, where he was an Associate Professor. In 1999, he joined the Department of Electronic Science and Engineering, Nanjing University, where he is currently a Professor. He has presided over and undertaken more than 30 national natural science foundation of China and Jiangsu province science and technology plan projects. He has published more than 100 academic papers and applied for/authorized more than 20 national invention patents. His research interests include target recognition and image processing.

Lan Tang received the B.S and M.S. degrees in communication engineering from the Jilin University, Jilin, China, in 2002 and 2005, respectively, and the Ph.D. degree in communication and information science from Southeast University, Nanjing, China, in 2009. Since 2009, she has joined the school of electronic science and engineering, Nanjing University, China, where she is now an associate professor. She has published many papers in IEEE TWC, IEEE TCOM, IEEE JSAC and other academic journals. As the project leader, she is currently undertaking a national fund project. Her current research interests include cooperative communication, energy efficient and energy harvesting wireless communication, wireless information and power transfer, and optimization theory.

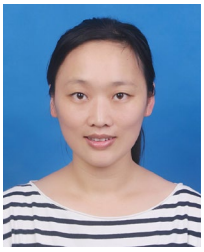

Qiong Wang received the B.S. and the Ph.D. degrees in Electronic Science and Engineering from PLA University of Science and Technology, China, in 2004 and 2011, respectively. Since 2014, she has been Lecturer at Nanjing University, China. She has published more than 20 academic papers, of which 14 were retrieved by SCI and EI. Her current research interests include target automatic recognition and radar target detection.